

# A green route to phytofabricated synthesis of *Gymnema sylvestre* conjugated silver nanoparticles (GS-AgNPs) and its antimicrobial activity

Sk Nurul Hasan,<sup>1</sup> Sarat Chandra Jana,<sup>1</sup> Subhankar Manna,<sup>2</sup> Aditi Dey,<sup>2</sup> Kanchana Wijesekera,<sup>3</sup> Somenath Roy,<sup>\*2</sup> Mayuri Napagoda<sup>\*3</sup> and Braja Gopal Bag<sup>\*1</sup>

<sup>1</sup>Department of Chemistry and Chemical Technology, Vidyasagar University, Midnapore 721102, West Bengal, INDIA  
Email: brajagb@mail.vidyasagar.ac.in

<sup>2</sup>Department of Human Physiology with Community Health, Vidyasagar University, Midnapore 721102, West Bengal, INDIA  
Email: sroy.vu@hotmail.com

<sup>3</sup>Department 1Department of Biochemistry, Faculty of Medicine, University of Ruhuna, Galle 80 000, Sri Lanka  
Email: mayurinapagoda@yahoo.com

Received: December 15, 2019 | Accepted: December 30, 2019 | Published online: January 03, 2020

The plant-derived chemicals present in the leaf extract of *Gymnema sylvestre* (LEGS) commonly known as “Gurmer” has been utilized for the synthesis of *Gymnema sylvestre* conjugated silver nanoparticles (GS-AgNPs) at room temperature without any auxiliary reducing and capping agents. Spherical shaped GS-AgNPs of 26.6 nm average diameters were observed. A selective dose dependent antimicrobial activity of the freshly synthesized GS-AgNPs on both gram-positive *Staphylococcus aureus* and gram-negative *Proteus vulgaris* strain showed the same minimum inhibitory concentration (MIC) value at 50 µg/mL, as revealed by *in-vitro* MIC assay. Zone inhibition study carried out by Disk agar diffusion (DAD) test showed that the GS-AgNPs is sensitive on both the bacteria cell having a comparatively better antimicrobial activity towards Gram-negative over Gram-positive bacteria. The synthesized GS-AgNPs showed very low toxic effect in normal human cells. Dichlorodihydrofluorescein diacetate (DCDHFDA) and ethidium bromide-acridine orange (EB-AO) staining studies revealed that the GS-AgNPs mainly produces Reactive Oxygen Species (ROS) by altering its electron transport chain (ETC) system and it leads to cell death or necrosis through apoptosis of bacterial cells.

**Keywords:** *Gymnema sylvestre*, green synthesis, silver nanoparticles, antimicrobial, *Proteus vulgaris*, *Staphylococcus aureus*.

## 1. Introduction

In recent years nanochemistry opens a new vista for their diversified application on the various fields of science and technological innovation. During the last few decades scientists pay more and more attention towards metal nanoparticles due to their extremely minuscule size and large surface to volume ratio which drastically change both the physical well as chemical properties compared to the bulk materials.<sup>1,2</sup> Consequently, they exhibited miscellaneous application on different fields such as catalyst, pharmaceutical, medical imaging, drug delivery<sup>3,4,5,6,7,8,9,10,11</sup> etc. Among the various metal nanoparticles silver nanoparticles (AgNPs) have elicited much interest due to its biological activity such as antimicrobial, antifungal, antiviral and anticancer activities.<sup>12,13,14,15</sup> Among these activities AgNPs were very much prompt and widely used as a bactericidal agent. A number of methods have been used for the synthesis of AgNPs but a simple, less expensive and greener process will be more effective for sustainable developments.<sup>16,17,18</sup> In recent trends researchers pay more attention on green synthesis of silver nanoparticles using the plant-derived phytochemicals which act as both reducing as well as stabilizing agents instead of hazardous and toxic synthetic chemicals.<sup>19,20</sup> The synthesis of various metal nano particles using different plant extracts has been reported in the recent past.<sup>21,22,23,24,25,26</sup> The green synthesis of AgNPs from the extracts of *Andrographis paniculata*,<sup>27</sup> *Azadirachta indica*,<sup>28</sup> *Vinca rosea*,<sup>29</sup> *Eriobotrya japonica*,<sup>30</sup> *Aloe vera*,<sup>31</sup>

*Pedaliium murex*,<sup>32</sup> *Salacia chinensis*,<sup>33</sup> *Moringa oleifera*,<sup>34</sup> *Eugenia jambolana*,<sup>35</sup> *Gymnema sylvestre*,<sup>36</sup> etc., have also been reported in recent time. *Gymnema sylvestre*, commonly known as “Gurmar” is a slow-growing plant collected from the Vidyasagar University campus, West Bengal and it is distributed throughout India. It is widely used as a folk medicine in the care of diabetes, dyspepsia, asthma, constipation, jaundice, eye complaints and haemorrhoids<sup>37,38,39</sup> etc.

The eruption of microbial diseases increasing exponentially due to the rapid growth of different pathogenic bacteria, is one of the major problems throughout the world.<sup>40,41</sup> The rapid propagation of these diseases creates an epidemic situation within a quick time interval. World-wide attempts are ongoing from various perspectives to abolish these microbial diseases. In recent years, phytochemical conjugated green synthesized AgNPs have shown outstanding results to kill the embarrassing bacteria cell selectively without much inauspicious effects on the normal viable cell.<sup>42,43,44</sup> Herein we report one-step synthesis of *Gymnema sylvestre* conjugated silver nanoparticles (GS-AgNPs) from the leaf extract of *Gymnema sylvestre* (LEGS) without any auxiliary reducing or stabilizing agents at room temperature. The synthesized GS-AgNPs were characterized by UV-visible Spectroscopy, HRTEM, EDX, SAED, XRD and dynamic light scattering (DLS) studies. A selective dose-dependent antimicrobial activity of the freshly synthesized GS-AgNPs on both Gram-positive *Staphylococcus aureus* and Gram-negative *Proteus vulgaris* strain showed the same MIC

value at 50  $\mu\text{g/mL}$ , as revealed by *in-vitro* MIC assay. The synthesized GS-AgNPs have minimal toxicity on normal human cells (lymphocytes). GS-AgNPs is sensitive on both the bacteria cell having a comparatively better antimicrobial activity towards Gram-negative over Gram-positive bacteria, as examined by zone inhibition studies. The mechanistic investigation carried out by DCDHFDA and EB-AO staining studies revealed that the GS-AgNPs mainly produces ROS by altering its ETC system and it leads to cell death or necrosis through apoptosis of bacterial cells.

## 2. Material and Methods

The details of reagents used, identification of polyphenolic compounds, separation of lymphocytes are discussed in the supporting information.

### 2.1. Ag (I) solution

$\text{AgNO}_3$  was purchased from SRL (Sisco Research Laboratory) and used without further purification.  $\text{AgNO}_3$  (17.4 mg) was dissolved in deionized water (10 mL) to obtain a 10.24 mM Ag(I) stock solution.

### 2.2. Preparation of the leaf extract of *Gymnema sylvestre*

The leaves of *G. sylvestre* were collected from the local area of Midnapore, West Bengal, India and identified at the Department of Botany and Forestry, Vidyasagar University, Midnapore. The leaves were dried in sunlight and pulverized by using a grinder. Finely powdered leaves of *G. sylvestre* (1.5 gm) was suspended in ethanol (7 mL) in a test tube, sonicated in an ultrasonicator bath for 45 mins and then centrifuged for 10 mins to obtain a clear supernatant. To know the concentration of the leaves extract, an aliquot of the clear supernatant (1 mL) was taken in a round bottom flask and the volatiles were removed under reduced pressure to afford a sticky solid (4.0 mg). Thus the concentration of the leaf extract was 4000  $\text{mg L}^{-1}$ .

### 2.3. Synthesis of Silver Nanoparticles

Aliquots of Ag (I) solution (0.2 mL, 10.24 mM each) were added drop-wise to the leaf extract solution taken in vials. A series of stable GS-AgNPs were synthesized by changing the concentration of the leaf extract from 500, 1000, 1500, 2000 to 2500  $\text{mg L}^{-1}$ . The concentration of Ag(0) and the total volume of the solution in each vial was fixed at 0.51 mM and 4 mL respectively. Surface Plasmon Resonance spectroscopy of the synthesized GS-AgNPs was carried out after 24 h of mixing between Ag(I) solution and the LEGS.

### 2.4. Characterization

TEM images, SAED and EDX of AgNPs were taken from the Technai G2 instrument. X-ray diffraction (XRD) patterns of the stabilized AgNPs were recorded in PAN alytical X'pert Pro with Cu-K $\alpha$  radiation ( $\lambda = 1.54 \text{ \AA}$ ). Mass spectra were recorded in Shimadzu GCMS QP 2100 Plus. UV-visible spectra were recorded in Shimadzu 1601 spectrophotometer. DLS Study was carried out by using Malvern Zetasizer Nano series (Model-Nano ZS90) to know the size distribution of GS-AgNPs.

### 2.5. Antibacterial activity determination (MIC value estimation)

To estimate the antibacterial activity of GS-AgNPs, the freshly prepared GS-AgNPs were treated with a different

concentration on the bacterial population. MIC (Minimum inhibitory concentration) was performed through the micro dilution method. In brief the 10  $\mu\text{L}$  bacteria containing  $10^6$  population were added to each tube containing 1mL Luria broth (Hi-media, India) and after that the different doses of the GS-AgNPs were added (before using sonication was performed to form the suspension of silver nano particles like dissolved solution). Positive control means the experiment conducted without GS-AgNPs. Negative control means without bacteria. All culturing tubes were allowed for 24 h in shaking incubator at 198 rpm and temperature maintained at  $37 \pm 2^\circ\text{C}$ . After incubation the MIC value was measured by inspection of the turbidity of the medium.

### 2.6. Disk agar diffusion (DAD)

Disk agar diffusion (DAD) test was performed to detect drug susceptibility of multi-drug resistance bacteria to green coated GS-AgNPs. In this experiment the bacterial population from a fresh culture for 4 h having  $10^6$  CFU/ mL (inoculated from a single colony) was allowed to grown on Mueller- Hilton agar plate. Disks of 6 mm filter paper were used for the antibiotic tests and were pre-allowed to absorb 10  $\mu\text{L}$  of GS-AgNPs and plant extract of 10  $\text{mg/mL}$ . Circular inhibition adjacent the disk (along with the disk) shows transparent and was measured for DAD result.

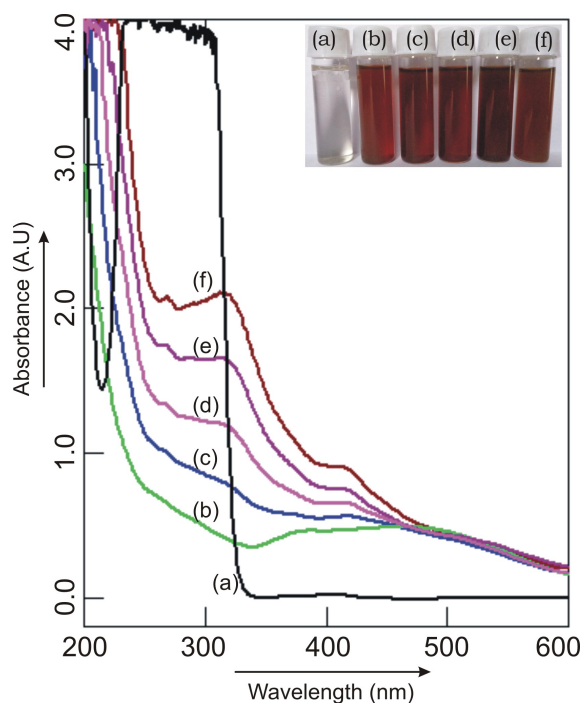


**Figure 1.** UV-visible spectra of (a)  $\text{AgNO}_3$  (0.51 mM), (b-f) AgNPs at 500, 1000, 1500, 2000 and 2500,  $\text{mg L}^{-1}$  concentrations of leaf extract respectively. Inset: Photograph of the vials containing (a)  $\text{AgNO}_3$  (0.51 mM) solution, (b-f) colloidal AgNPs at 500, 1000, 1500, 2000, and 2500  $\text{mg L}^{-1}$ . respectively (after 24 h of mixing).

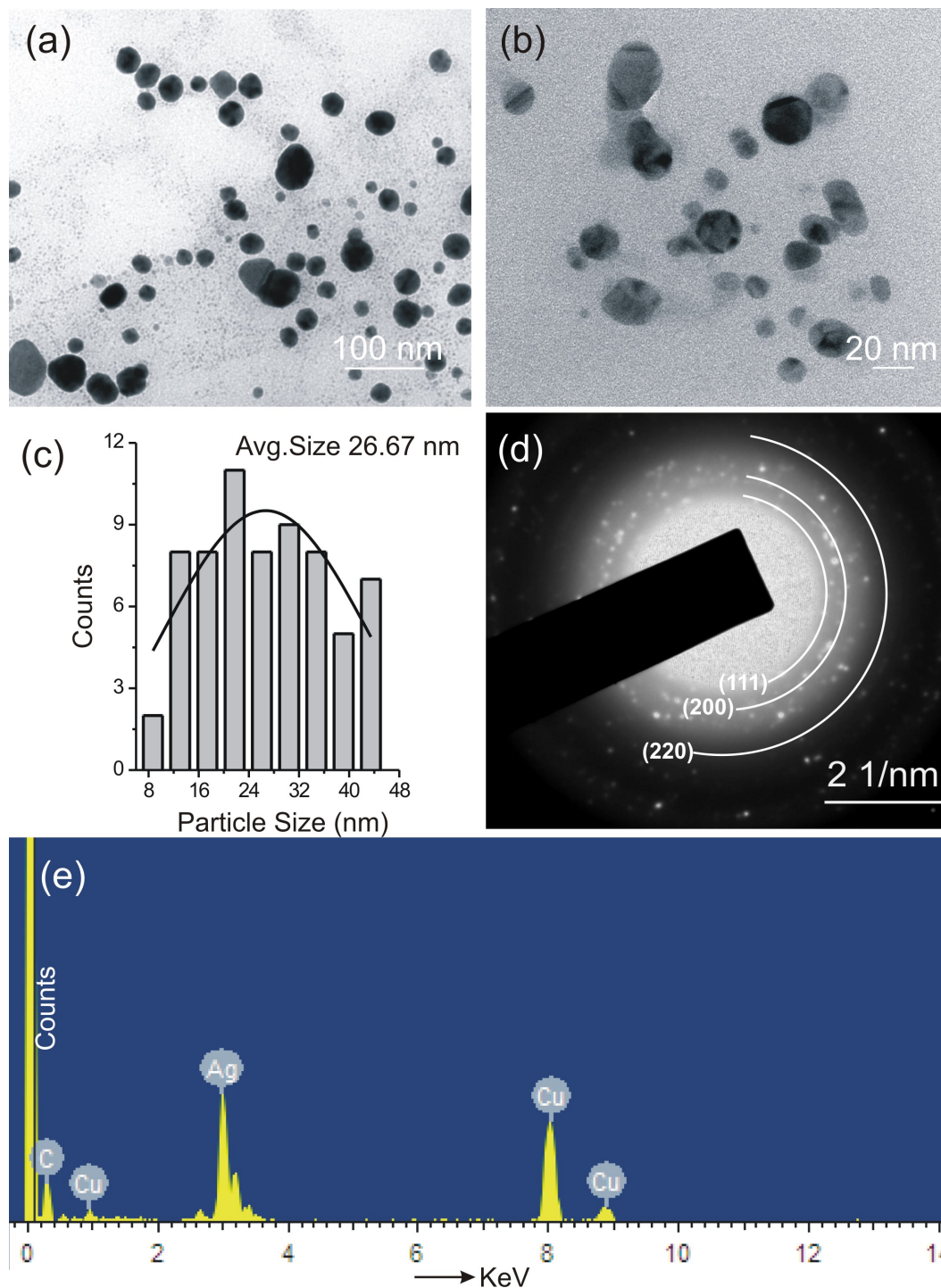


**Figure 2.** HRTEM Images of AgNPs obtained from the LEGS at  $500 \text{ mgL}^{-1}$ (a,b); (c) Histogram at  $500 \text{ mgL}^{-1}$  (average diameter 26.67 nm); (d) SAED image of stable AgNPs; (e) EDX image of stable GS-AgNPs.

### 2.7. Intracellular reactive oxygen species (ROS) measurement

Intracellular ROS measurement was performed using Dichloro dihydro fluorescein diacetate (DCDHFDA) according to the previously reported method.<sup>15</sup> In brief,

*P. vulgaris* ( $10^6$  cells/mL) was treated with GS-AgNPs and the plant particles at  $100 \mu\text{g/mL}$  for 24 h. After that specified treatment schedule cells were washed with culture media followed by incubation with  $1 \mu\text{g/mL}$  DCDHFDA for 30 min at  $37^\circ\text{C}$ . Then the cells were washed three times with fresh

culture media. The imaging of DCDHFDA stained cells was pictured in Nikon fluorescence microscope.

### 2.8. Apoptosis study by EtBr-AO staining

Apoptosis was done according to previously reported method<sup>15</sup> with some modification. Briefly, the bacterial cells were transferred to a 15 mL tube. Cells were pelleted by centrifuged at 2,500 rpm for 5 min and washed with 1 mL of cold PBS once. Cell pellets were then re-suspended in 25  $\mu$ L cold PBS and 5  $\mu$ L Ethidium bromide-Acridine Orange mixture (EB-AO, 20  $\mu$ g/mL) stain was added. Stained cells suspension (20  $\mu$ L) were placed on a clean microscope slide and covered with a cover slip. Cells were viewed and counted using a phase-contrast fluorescence inverted microscope at 400 $\times$  magnification with excitation filter 480/30 nm. Pictures were taken with a Nikon digital camera of Nikon ECLIPSE LV100POL phase contrast fluorescence microscope. Tests were done in triplicate, counting a minimum of 100 total cells each.

## 3. Results and Discussion

The different types of plant-derived phytochemical such as triterpene saponins, steroids, alkaloids, flavones including polyphenolic compounds are present in the LEGS.<sup>45,46</sup> Mass spectrum of the LEGS strongly supported the abundance of most of these compounds (supporting information Figure S1). In our ongoing efforts on the practical application of terpenoids (C30s) as a useful biocompatible nano entities,<sup>47,48,49,50,51,52</sup> the evidence for the presence of large amount of polyphenolic compounds present in LEGS along with its biological activities inspired us to investigate its usefulness in the synthesis of AgNPs from AgNO<sub>3</sub>.<sup>28,31</sup>

### 3.1. Synthesis of AgNPs and study of its Surface Plasmon Resonance spectroscopy

The phytochemicals including polyphenols have been extensively utilized for the facile synthesis of silver nanoparticles via green route at room temperature.<sup>20,42</sup> However, to our knowledge, LEGS has not been utilized for the green synthesis of AgNPs. In a typical experiment, we mixed the Ag(I) solution with aqueous solutions of the LEGS taken in vials (Figure 1). Appearance of light red coloration after 45 mins confirmed the formation of GS-AgNPs. The intensification of the color of the solutions with time was observed on keeping the solutions at room temperature for 24 h and then no further change in color was observed indicating the formation of stable GS-AgNPs.

### 3.2. Synthesis HRTEM, XRD, EDX, SAED and DLS studies

To understand the structural properties such as morphology, shape and size distribution of nanoparticles in the crystal lattice we carried out the High-Resolution Transmission Electron Microscopy (HRTEM) of the GS-AgNPs. Mostly spherical shaped AgNPs were observed with an average particle size of 26.67 nm at 500 mgL<sup>-1</sup> concentration of the leaf extract (Figure 2a-c). The elemental composition of the synthesized GS-AgNPs was determined

by energy dispersive X-ray analysis (EDX). The presence of Ag-peak along with 'C' coming from the stabilizing organic ligands confirmed the formation of GS-AgNPs (Figure 2e). The samples were coated over a glass plate, and X-ray diffraction analysis of the *G. sylvestre* conjugated AgNPs (GS-AgNPs) was carried out after removal of the volatiles. X-ray diffraction pattern of the GS-AgNPs was given in (Figure 3). Amorphous nature of the metallic fcc lattice of GS-AgNPs was proved from the characteristic reflections of the planes (111), (200), (220), and (311) at  $2\theta = 38.1^\circ$ ,  $44.5^\circ$ ,  $64.5^\circ$ , and  $77.5^\circ$  respectively. The predominant orientation of the (111) was supported by a comparatively larger peak intensity of this plane with respect to the other planes. These values are in agreement with the reported standards JCPDS file no. 04-0783. Selected area electron diffraction (SAED) pattern obtained from a GS-AgNPs (Figure 2d) showed the diffraction rings from inner to outer associated with the (111), (200) and (220) atomic planes of silver indicating the formation of silver nanoparticles.

DLS studies of stable GS-AgNPs obtained from the LEGS were carried out at 500 mgL<sup>-1</sup>, 1000 mgL<sup>-1</sup>, 1500 mgL<sup>-1</sup> and 2000 mgL<sup>-1</sup> concentrations of the leaf extract. The average hydrodynamic diameters of stable GS-AgNPs increased with increasing the concentration of the leaf extract. This is due to the presence of larger number of ligands on the surface of GS-AgNPs with increasing the concentration of leaf extract (supporting information S2). The polydispersity index (PDI) of the synthesized GS-AgNPs were in the range of 0.33 to 0.55 indicated that the silver nanoparticles does not possess the uniform size. HRTEM

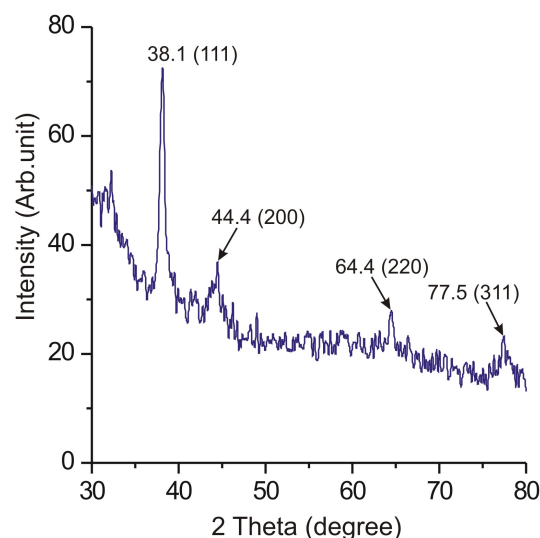


**Figure 3.** XRD of stable silver nanoparticles (GS-AgNPs) obtained from the LEGS.

images also supported this observation.

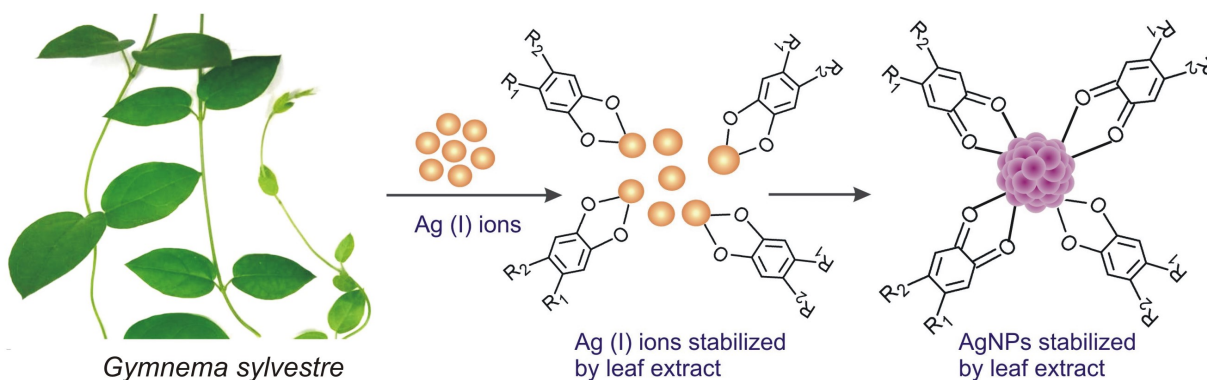


**Figure 4.** Mechanism of the origination and stabilization of GS-AgNPs by the phytochemicals present in the LEGS.

#### 4. Mechanism of the formation of Stabilized GS-AgNPs

Mass spectrum of the LEGS supported the abundance of different types of phytochemicals including triterpene saponins, polyphenols, alkaloids, flavones, steroids etc. (supporting information Figure S1). Taking a *o*-dihydroxy compound as a reducing as well as stabilizing agent present in the leaf extract, we propose a mechanism for the formation and stabilization of stable GS-AgNPs (Figure 4). The details of the plausible mechanistic explanation were discussed in supporting information section 3.<sup>53, 54</sup>

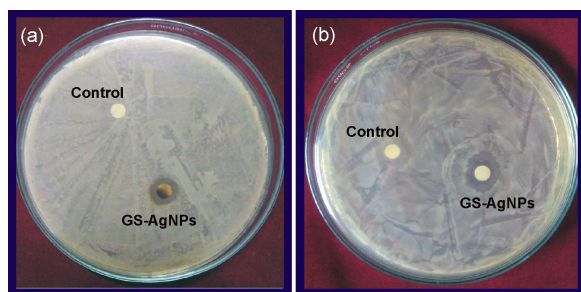


**Figure 5.** Antibacterial activity of GS-AgNPs against bacterial strains: (a) Gram-positive *Staphylococcus aureus* (b) Gram-negative *proteus vulgaris*.

#### 5. Antimicrobial activity of Stabilized AgNPs

The antimicrobial activity of the freshly synthesised GS-AgNPs and plant extract was carried out against both Gram-positive *S. aureus* and Gram-negative *P. vulgaris* strain at different concentrations. The GS-AgNPs showed strong dose dependent antimicrobial activity whereas no such significant effect was found in the case of plant extract at higher dose (100  $\mu\text{g/mL}$ ). MIC is the lowest concentration of the GS-AgNPs which can inhibit the visible growth of micro-organism. The MIC value (a particular concentration where no visible growth or turbidity appears) of GS-AgNPs measured against both *S. aureus* and *P.vulgaris* strain was 50  $\mu\text{g/mL}$  (supporting information Figure S3 and S4). The antimicrobial susceptibility test using disk agar diffusion is well-known method to know the antimicrobial activity of synthesized nano particles. Silver nano particles have

significant antimicrobial activity because it can damage the DNA of the bacterial cell and also prevent the rapid reproduction of the bacterial cells. The antimicrobial activity of GS-AgNPs was studied by DAD tests, freshly prepared colloidal GS-AgNPs showed extensive growth inhibition on *S. aureus* as well as *P.vulgaris* strain proving by the formation of inhibition zones of  $10 \pm 0.5$  mm and  $16 \pm 0.6$  mm respectively at a selective dose of 50  $\mu\text{g/mL}$  (Figure 5). In the case of plant extract, no significant change of inhibition zones was observed at the same dose. The circumference of the inhibition zones indicated that the GS-AgNPs exhibits more bactericidal activity on Gram negative *P. vulgaris* compared to the Gram positive *S. aureus*. The reason for such a difference in bactericidal effects towards gram negative and gram positive bacteria might be due to the difference in permeability of the respective cell membranes. The synthesized GS-AgNPs showed very low toxic effect in normal human cells (Lymphocytes), with step-wise increase in the dose concentration of GS-AgNPs from 1  $\mu\text{g/mL}$  to 5  $\mu\text{g/mL}$ , 10  $\mu\text{g/mL}$ , 25  $\mu\text{g/mL}$ , 50  $\mu\text{g/mL}$  and 100  $\mu\text{g/mL}$ , the percentage of viable human lymphocytes are 95.8%, 93.8%, 89.1%, 85.3%, 82.4% and 78.8% respectively (Figure 6). From these results it was clear that the GS-AgNPs have potential to resist the microbial growth without much harmful effects on the normal viable lymphocytes and 100  $\mu\text{g/mL}$  or its lower does can be used as a safe concentration for biological purpose.<sup>15,55</sup>

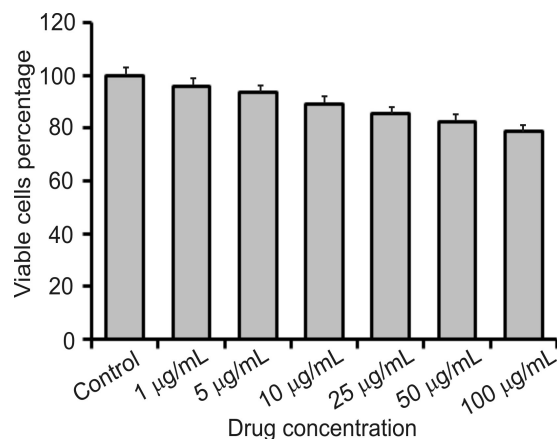


**Figure 6.** Viable cells vs concentration plot of GS-AgNPs synthesized from the LEGS.

Generally silver nano particles have a high affinity to interact with DNA and regulatory enzymes of the bacterial system. Silver nano-particles also have a tendency to leakage the outer membrane of the bacterial system. As a result, silver nano-particles can enter the inner cell membrane of the bacteria that can produce ROS and inhibiting the growth of the cells. The freshly synthesized colloidal GS-AgNPs cause the mitochondrial disruption by ROS generation (hydroxyl radical, thiol radical, carbonate radical, nitroxide radical etc.) which oxidized the DCFH<sub>2</sub>DA to fluorescence active compound Dichloro fluorescein (DCF). The intensity of fluorescence microscopic images indicated that the GS-AgNPs elevate the level of ROS generation and consequently increase the active DCF compound in bacterial cells compared to the plant extract (control) at 50 µg/mL does (figure 7b-e).

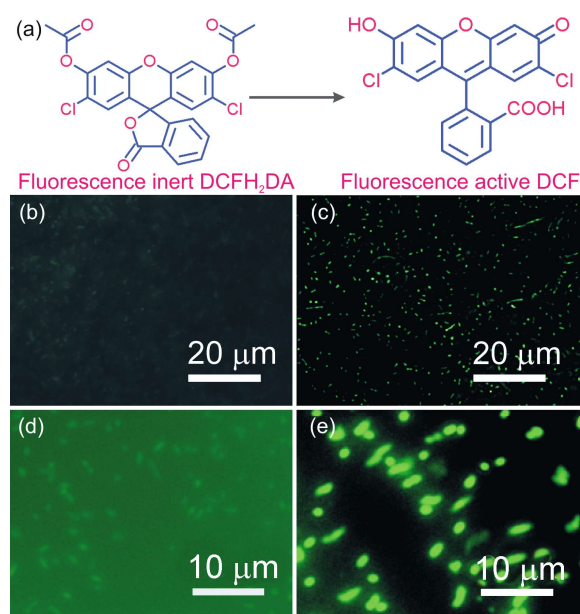


**Figure 7.** (a) Oxidation of DCFH<sub>2</sub>DA to DCF by ROS generation; ROS generation micrographs against the *Staphylococcus aureus* bacterial cell (b) for control, (c) for treated GS-AgNPs; ROS generation micrographs against the *Proteus vulgaris* bacterial cell (d) for control, (e) for treated GS-AgNPs.

Ethidium Bromide (EtBr) binds with the DNA of the bacterial cell and Acridine Orange (AO) is a color specific fluorescent. AO stains the live bacterial cells whereas EtBr stains only the bacterial dead cells. This double staining process can help to detect the live or dead cells after the treatment with GS-AgNPs. In EtBr-AO staining studies, increases of orange colour for *S. aureus* and yellowish colour for *P. vulgaris* bacterial cells population revealed that the GS-AgNPs caused apoptosis in bacterial cells beside this also elevated necrotic cell population at significant level. Whereas in case of plant extract (control) it seems that there is no significant changes and the cells remain in greenish colour (Figure 8a-d). So this study indicates that most of the cell death occurred principally through apoptosis.<sup>15,56,57,58</sup>

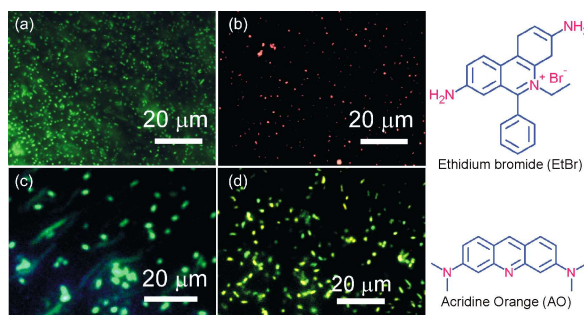


**Figure 8.** EtBr-AO staining micrographs against the *Staphylococcus aureus* cell (a) for control, (b) for treated GS-AgNPs; EtBr-AO staining micrographs against the *Proteus vulgaris* cell (c) for control, (d) for treated GS-AgNPs.

## 6. Conclusion

Colloidal silver nanoparticles of 26.6 nm average diameters were synthesized using the LEGS in water at room temperature. Taking a polyphenolic phytochemical as a model compound present in LEGS, a plausible mechanism for the formation and stabilization of silver nanoparticles (GS-AgNPs) has been proposed. The *in-vitro* antimicrobial activity of the phyto-fabricated AgNPs on both Gram-positive *S. aureus* and Gram-negative *p. vulgaris* strain was demonstrated. The GS-AgNPs showed better antimicrobial activity on Gram-negative *p. vulgaris* bacteria over the Gram-positive bacteria *S. aureus*. The synthesized GS-AgNPs showed a very low toxic effect in normal cells up to a concentration level of 100 µg/mL. From these results it can be concluded that, the 100 µg/mL or its lower does i.e. 50 to 100 µg/mL can be used as a safe concentration for biological use. Further *in-vivo* studies are in progress in our laboratory.

## 7. Acknowledgement

BGB thanks Science and Engineering Research Board (SERB) India (EMR/2017/000069), **India-Srilanka** project (DST/INT/SL/P25/2016), New Delhi, and Vidyasagar University for financial support and infrastructural facilities. SNH thanks UGC to provide research fellowships. Miss Aditi Dey thanks to the DST for research assistance [DST/INSPIRE Fellowship/2015/IF 150762].

## 8. References

1. A. M. Alkilany, S. E. Lohse, C. J. Murphy, *Acc Chem Res*, **2013**, 46, 650-661.
2. S. A. Aromal, D. Philip, *Spectrochim. Acta A*, **2012**, 97, 1-5.
3. C. J. Murphy, A. M. Gole, J. W. Stone, P. N. Sisco, A. M. Alkilany, E. C. Goldsmith, S.C. Baxter, *Acc Chem Res*, **2008**, 41,1721-1730.
4. K. G. Thomas, P. V. Kamat, *Acc Chem Res*, **2003**, 36, 888-898.
5. N. L. Rosi, C. A. Mirkin, *Chem Rev.*, **2005**, 105, 1547-1562.
6. M. M. R. Mollick, B. Bhowmick, D. Maity, D. Mondal, M. K. Bain, K. J Bankura, S. oy, D. Rana, K. Acharya, D.

- Chattopadhyay, *International Journal of Green Nanotechnology*, **2012**, 4, 230-239.
7. G. F. Paciotti, L. Myer, D. Weinreich, D. Goia, N. Pavel, R. E. McLaughlin, L. Tamarkin, *Drug Delivery*, **2004**, 11, 169-183.
  8. V. S. Kotakadi, S. A. Gaddam, S. K. Venkata P. V. G. K. Sarma, D. V. R. S. Gopal, *Biotech*, **2016**, 6, 216.
  9. P. Ghosh, G. Han, M. De, C. K. Kim, V. M. Rotello, *Adv Drug Delivery Rev*, **2008**, 60, 1307-1315.
  10. C. D., Pina, E. Falletta, M. Rossi, *Chem Soc Rev*, **2012**, 41, 350-369.
  11. A. Panacek, R. Prucek, J. Hrbac, T. Nevecna, J. Steffkova, R. Zboril, L. Kvitek, *Chem Mater*, **2014**, 26, 1332-1339.
  12. Z. Xiu, Q. Zhang, H. L. Puppala, V. L. Colvin, P. J. J. Alvarez, *Nano Lett*, **2012**, 12, 4271-4275.
  13. S. Eckhardt, P. S. Brunetto, J. Gagnon, M. Priebe, B. Giese, K. M. Fromm, *Chem Rev*, **2013**, 113, 4708-4754.
  14. V. S. Kotakadi, S. A. Gaddam, S. K. Venkata D. V. R. S. Gopal, *Current NanoScience*, **2015**, 15, 525-531.
  15. B. Das, S. K. Dash, D. Mandal, J. Adhikary, S. Chattopadhyay, S. Tripathy, *J Health Sci*, **2016**, 1, 89-101.
  16. S. Iravani, *Green Chem*, **2011**, 13, 2638.
  17. V. S. Kotakadi, S. A. Gaddam, S. K. Venkata, D. V. R. S. Gopal, *Appl Nanosci* doi:10.1007/s13204-014-0381-7 **2014**.
  18. J. A. Dahl, B. L. S. Maddux, J. E. Hutchison, *Chem Rev*, **2007**, 107, 2228-2269.
  19. J. M. Campelo, D. Luna, R. Luque, J. M. Marinas, A. A. Romero, *ChemSusChem*, **2009**, 2, 18-45.
  20. K. Jadhav, S. Deore, D. Dhamecha, H. R. Rajeshwari, S. Jagwani, S. Jalalpure, R. Bohara, *ACS Biomater Sci Eng*, **2018**, 4, 892-899.
  21. S. O. Aisida, N. Madubuonu, M. H. C. Alnasir, I. Ahmad, S. Botha, M. Maaza, F. I. Ezema, *Applied Nanoscience* doi.org/10.1007/s13204-019-01099-x
  22. A. Parmar, G. Kaur, S. Kapil, V. Sharma, R. Sandhir, S. Sharma, *Applied Nanoscience*, **2019**, 9, doi.org/10.1007/s13204-019-01108-z2017
  23. A. C. Barai, K. Paul, A. Dey, S. Manna, S. Roy, B. G. Bag, C. Mukhopadhyay, *Nano Convergence*, **2018**, 5, 1-9.
  24. J. R. Nakkala, R. Mata, E. Bhagat, S. R. Sadras, *J. Nanopart. Res.*, **2015**, 17, 1-15.
  25. K. Chaudhuri, S. N. Hasan, A. C. Barai, S. Das, T. Seal, B. G. Bag, *Journal of Pharmacognosy and Phytochemistry*, **2018**, 7, 1434-1442.
  26. K. Chaudhuri, S. N. Hasan, A. C. Barai, S. Das, T. Seal, B. G. Bag, *The Pharma Innovation Journal*, **2018**, B, 437-446.
  27. S. K. Venkata, Y. S. Rao, S. A. Gaddam, T. N. V. K. V. Prasad, V. Reddy, D. V. R. S. Gopal, *European Journal of Medicinal chemistry*, **2014**, 73, 135-140.
  28. K. Ramar, V. Vasanthakumar, A. Priyadharsan, P. Priya, V. Raj, P. M. Anbarasan, R. Vasanthakumari, A. J. Ahamed, *Journal of Materials Science*, **2018**, 29, 11509-11511.
  29. S. K. Venkata Y. S. Rao, S. A. Gaddam, T. N. V. K. V. Prasad, V. Reddy, D. V. R. S. Gopal, *Colloids Surf. B: Biointerfaces*, **2013**, 105, 194-198.
  30. B. Rao, R. C. Tang, *Adv Nat Sci Nanosci Nanotechnol*, **2017**, 8, 015014.
  31. P. Tippayawat, N. Phromviyo, P. Boueroy, A. Chompoosor, *Peer J*, **2016**, DOI 10.7717/peerj.2589.
  32. K. Anandalakshmi, J. Venugobal, V. Ramasamy, *Appl Nanosci*, **2016**, 6, 399-408.
  33. K. Jadhav, S. Deore, D. Dhamecha, H. R. Rajeshwari, S. Jagwani, S. Jalalpure, R. Bohara, *ACS Biomater Sci Eng*, **2018**, 4, 892-899.
  34. S. O. Aisida, E. Ugwoke, A. Uwais, C. Iroegbu, S. Botha, I. Ahmad, M. Maaza, F. I. Ezema, *Journal of Polymer Research*, **2019**, 26, 1-11.
  35. A. Parmar, G. Kaur, S. Kapil, V. Sharma, S. Sachar, R. Sandhir, S. Sharma, *Reactive and Functional Polymers*, **2019**, 141, 68-81.
  36. S. S. Pingale, S. V. Rupanar, M. Chaskar, *Journal of Water and Environmental Nanotechnology*, **2018**, 3,106-115.
  37. S. K. Mitra, S. Gopumadhavan, T. S. Muralidhar, S. D. Anturlikar, M. B. Sujatha, *Indian J. Exp. Biol.*, **1995**, 33, 798-800.
  38. V. G., Khanna, K. Kannabiran, G. Rajakumar, A. A. Rahuman, T. S. kumar, *Res.*, **2011**, 109, 1373-1386.
  39. A. Saneja, C. Sharma, K. R. Aneja, R. Pahwa, *Pharm Lett.*, **2010**, 2, 275-284.
  40. T. T. Yoshikawa, *J Infect Dis*, **1997**, 176, 1053-7.
  41. K. P. High, *Lancet Infect Dis*, **2002**, 2, 655.
  42. S. Islam, B. S. Butola, F. Mohammad, *RSC Adv*, **2016**, 6, 44232-44247.
  43. M. Ehsan, T. Yazdi, J. Khara, H. R. Sadeghnia, S. E. Bahabadi, M. Darroudi, *Res Chem Intermed*, **2018**, 44, 1325-1334.
  44. U. B. Jagtap, V. A. Bapat, *J Plant Biochem Biotechnol*, **2013**, 22, 434-440.
  45. S. Vaidya, *pharmacia1*, **2011**, 37, 42.
  46. W. Ye, X. Liu, Q. Zhang, C. T. Che, S. Zhao, *J Nat Prod*, **2011**, 64, 232-235.
  47. B. G. Bag, R. Majumdar, *Chem Rec*, **2017**, 17, 1-34.
  48. B. G. Bag, R. Majumdar, *RSC Adv.*, **2014**, 4, 53327-53334.
  49. B. G. Bag, S. Das, S. N. Hasan, A. C. Barai, *RSC Adv*, **2017**, 7, 18136.
  50. B. G. Bag, S. N. Hasan, P. Pongpamorn, N. Thasana, *ChemistrySelect*, **2017**, 2, 6650- 6657.
  51. B. G. Bag, S. N. Hasan, S. Ghorai, S. K. Panja, *ACS Omega*, **2019**, 4, 7684-7690.
  52. B. G. Bag, A. C. Barai, K. Wijesekera, P. Kittakoop, *ChemistrySelect*, **2017**, 2, 4969 – 4973.
  53. C. Garai, S. N. Hasan, A. C. Barai, S. Ghorai, S. K. Panja, B. G. Bag, *Journal of Nanostructure in Chemistry*, **2018**, 8, 465-472.
  54. K. Chaudhuri, S. N. Hasan, A. C. Barai, S. Das, T. Seal, B. G. Bag, *Asian Journal of Pharmacy and Pharmacology*, **2019**, 5, 332-343.
  55. B. Das, S.K. Dash, D. Mandal, T. Ghosh, S. Chattopadhyay, S. Tripathy, *Arabian J Chem* Doi: 10.1016/j.arabjc. **2015**.08.008
  56. S.K. Dash, T. Gosh, S. Roy, S. Chottopadhyay, D, Das, *J. Appl. Toxicol*, **2014**, 34, 1130-1144.
  57. N. Miura, Y. Shinohara, *Biochemical and Biophysical Research Communications*, **2009**, 390, 733-737.
  58. H. Bao, X. Yu, C. Xu, X. Li, Z. Li, D. Wei, Y. Liu, *PLOS One*, **2015**, 10, 1-10.